EUROPEAN ORGANIZATION FOR NUCLEAR RESEARCH

Proposal to the ISOLDE and Neutron Time-of-Flight Committee

Lattice sites, charge and spin states of Fe in $In_xGa_{1-x}N$ studied with emission Mössbauer spectroscopy

October 06, 2016

H. Masenda[1], H. P. Gunnlaugsson[2], D. Naidoo[1], K. Bharuth-Ram[3], R. Mantovan[4], H. P. Gíslason [5], A. Bonanni[6], A. Tarazaga[6], A. Vantomme[2], K. Johnston[7], J. Schell[7], B. Qi[5], S. Ólafsson[5]

[1]*School of Physics, University of the Witwatersrand, 2050, South Africa*

[2]*Instituut voor Kern-en Stralings fysika, KU Leuven, B-3001 Leuven, Belgium*

[3]*School of Physics, Durban University of Technology, Durban 4000, South Africa*

[4]*Laboratorio MDM, IMM-CNR, Via Olivetti 2, I-20864 Agrate Brianza (MB), Italy*

[5]*Science Institute, University of Iceland, Dunhaga 3, IS-107 Reykjavík, Iceland*

[6]*Institute for Semiconductor and Solid State Physics, Nitride Compound Semiconductor Group, Johannes Kepler University, Altenbergerstr. 69, Linz, Austria*

[7]*EP Department, ISOLDE/CERN, 1211 Geneva 23, Switzerland*

Spokesperson(s): H. Masenda (hilary.masenda@wits.ac.za), H. P. Gunnlaugsson (HPGunnlaugsson@gmail.com)

Local contact(s): K. Johnston (karl.johnston@cern.ch), J. Schell (Juliana.schell@cern.ch)

CERN-INTC-2016-055 / INTC-P-485
07/10/2016

Abstract

Ternary group III-nitrides have been the focus of intensive research over the past few decades due to the possibility of tuning their unique physical properties such as the energy band gap, effective masses of holes and electrons, and dielectric constants. This has opened a range of applications, spanning from commercial full colour light emitting diodes, laser diodes, solar cells to high power field effect transistors.

In our previous experiment (IS576) we have investigated the charge states of Fe in $Al_xGa_{1-x}N$, where it has been demonstrated that we can follow the effect of doping on the charge states of Fe and the interactions of Fe with point defects in the material using highly dilute implantations of ^{57}Mn ($T_{½}$ = 1.5 min.).

Test experiments with InN show completely different behaviour from the $Al_xGa_{1-x}N$ (including GaN, x=0), suggesting different physics in the two systems that are currently not understood. It is possible that the implantation process creates defects that are either spin-polarized and/or acceptors, properties that are of interest in further development of this system for technological applications.

We propose here experiments utilizing ^{57}Mn ($T_{½}$ = 1.5 min.) and ^{57}Co ($T_{½}$ = 272 d) for ^{57}Fe emission Mössbauer spectroscopy to study the $In_xGa_{1-x}N$ system in detail, and to determine an understanding of the effect of the implantation process and/or post treatment on the material.

Requested shifts: 10 shifts, (split into ~2-3 runs over ~3 years)

1 INTRODUCTION

InGaN is a direct bandgap ternary semiconductor derived from two binary III-nitrides, InN and GaN, which is stable in the wurtzite structure [1]. The significance of InGaN alloys as active layers in optoelectronic and photovoltaic devices is illustrated in Fig 1. By tuning the relative abundance of Ga and In, it is possible to engineer the band gap of $In_xGa_{1-x}N$. Recently, optoelectronic devices based on ternary semiconducting $In_xGa_{1-x}N$ alloys operating across the visible spectrum stemming from energy bandgap ranging from the ultraviolet ($E_{g\ GaN}$ = 3.51 eV [2]) to the infrared ($E_{g\ InN}$ = 0.7 eV [3]) have been commercialized. Examples include: employment of light emitting diodes and laser diodes in traffic lights, full-colour displays, backlighting sources for liquid-crystal displays, general lighting and high definition "Blu-ray" disc read-heads all of which utilise an $In_xGa_{1-x}N$ blue-violet laser [4,5,6]. Duly recognising its technological usefulness is the award of the 2014 Nobel Prize in Physics for "*the invention of efficient blue light emitting diodes which has enabled bright and energy saving white light sources*" [7]. These diodes are based on $In_xGa_{1-x}N$ active layers as indispensable components.

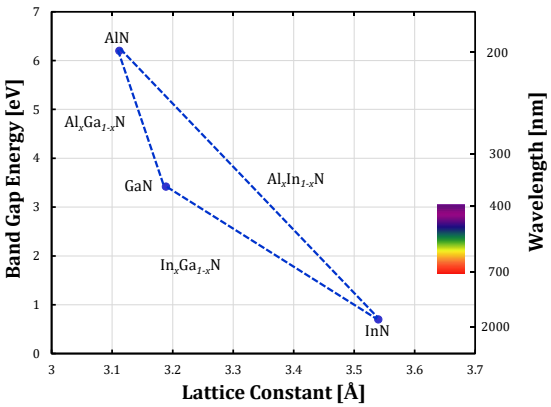

Fig 1: Bandgap energy at room temperature vs lattice constants for III-nitride semiconductors.

Over the years, the exploitation of these alloys in optoelectronic devices and photovoltaics has been hampered by challenges imposed by the necessity of increasing the indium content [8]. This increase, coupled with the lattice mismatch between the InGaN and GaN substrates generate defects which in turn compromise the efficiency of these alloys in optoelectronic systems [9]. However, despite the large crystal defect densities, $In_xGa_{1-x}N$ still exhibits high LED efficiency compared to other semiconductors, the cause of which is still unknown [4,10]. Localised states in the $In_xGa_{1-x}N$ active layer have been proposed [11,12,13], although their origin and whether they are indeed responsible for the high efficiency is not yet clear [4]. Similar to the binary constituents, GaN and InN, a critical issue has been *p*-type doping in $In_xGa_{1-x}N$ since the introduction of metallic elements such as Zn and Mg during growth has been observed to hinder acceptor doping due to the formation of complexes with hydrogen. Post-deposition thermal annealing in order to dissociate these complexes has proven useful in enhancing the release of free holes [14,15]. In spite of $In_xGa_{1-x}N$ (mostly Ga rich) being used in actual commercial devices, basic knowledge of dopant lattice sites, their charge states and the formation of defects tin $In_xGa_{1-x}N$ is still required to improve the efficiency/lifetime of current devices and expand its range of applications.

Motivation - previous studies

The experiments proposed here are motivated by the results from our previous experiments, IS501: *Emission Mössbauer spectroscopy of advanced materials for opto- and nano- electronics* [16] and IS576: *Magnetic and structural properties of manganese doped (Al,Ga)N studied with emission Mössbauer spectroscopy* [17]. As part of IS501, we studied the potential magnetic effects of Fe impurities in GaN following ^{57}Mn* implantation in the temperature range, 100 – 800 K. The room temperature spectrum shown in Fig 2 was analysed in terms of two spectral components with the following assignments:

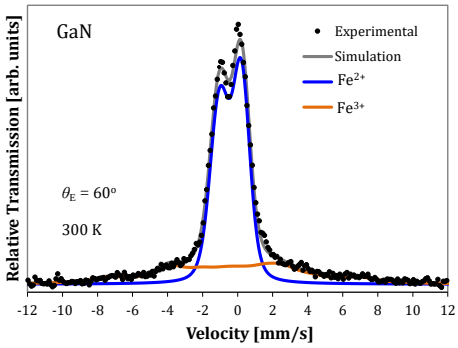

Fig 2: eMS spectrum of GaN obtained at 300 K and at an emission angle (θ_E) of 60°.

- Fe^{3+}: High-spin Fe^{3+} on substitutional Ga sites showing slow paramagnetic relaxations, evident as magnetic structure on the wings of the spectra as observed in ZnO [18].

- Fe^{2+}: High-spin Fe^{2+} on substitutional Ga sites, where the Fe^{2+} state is stabilized by nitrogen vacancies [19]. The Fe^{2+} shows considerable effects of covalency.

Following on from IS501, in the IS576 experiment, we have investigated the lattice sites, charge states and magnetic behaviour of Fe in virgin and Mn doped $Al_xGa_{1-x}N$ films, for x = 0.12, 0.20, 0.40, 0.60 and 0.80. Final data analysis and comparison with theoretical calculations is currently in progress and manuscripts are being prepared for publication. Room temperature spectra measured at 60° and 0° for AlGaN samples with 20% Al content and with and without 1% Mn doping are shown in Fig 3. As in GaN (x = 0), similar results were obtained for non-Mn doped $Al_xGa_{1-x}N$ samples. For Mn doped samples a marked reduction in the magnetic distribution component due to Fe^{3+} is observed and it was necessary to include an additional single line component to fit the data. On the basis of its isomer shift, the single line component is assigned to:

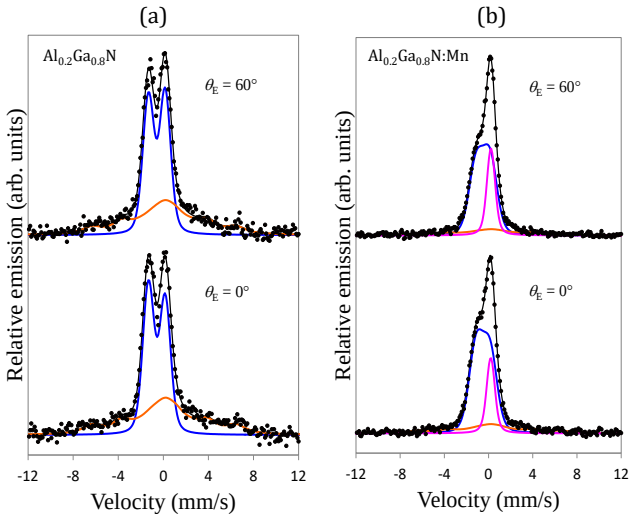

Fig 3: Selected Mössbauer spectra obtained for (a) virgin and (b) 1% Mn pre-doped $Al_{0.2}Ga_{0.8}N$ with at emission angle (θ_E) indicated.

- Fe^{4+} which seems to compensate for the high spin Fe^{3+} contribution while the relative area fraction of Fe^{2+} (S=2) compared with the equivalent un-doped sample with similar Al/Ga concentrations is maintained.

One of the objectives of the above study (IS576) was to ascertain the effect of acceptor doping with Mn in these nitrides. The coexistence of a sufficient number of magnetic dilute ions and free holes above the insulator-to-metal transition is a requirement in the theoretical model of Dietl *et al.* [20,21] for the realization of carrier mediated dilute magnetism.

The spectrum from a test eMS measurement on InN is shown in Fig 4. The spectrum clearly reveals significant differences compared to $Al_xGa_{1-x}N$ (including, GaN, x = 0), which forms the basis of the experiments proposed herein.

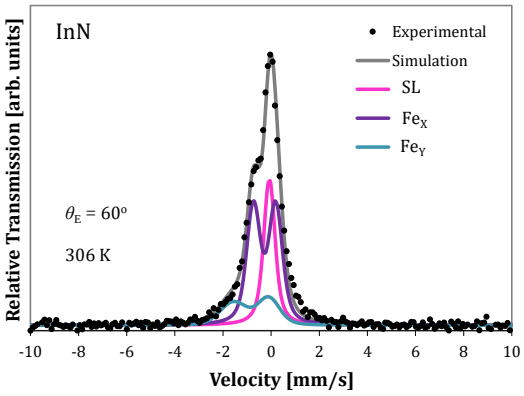

Fig 4: ^{57}Fe emission Mössbauer spectrum obtained at 306 K for InN after implantation of $^{57}Mn^*$ at $\theta_E = 60^o$.

Preliminary analysis of the InN data required three spectral components and their tentative assignments are discussed in detail below, together with a comprehensive description of these differences and the prospective experiments required to fully understand the findings we observe in these materials.

1. There is no magnetic structure on the wings of the spectrum, as observed in $Al_xGa_{1-x}N$ (see Fig. 3 (a)), suggesting the absence of high spin Fe^{3+} in InN. Instead, there is a single line which is attributable to Fe^{4+} similar to Mn pre-doped $Al_xGa_{1-x}N$. This could be interpreted as a consequence of acceptor defects created in the implantation process and suggest an alternative way of obtaining *p*-type doping in this system.
2. The straightforward interpretation of the quadrupole-split doublet (Fe_X) with reference to the results obtained in the $Al_xGa_{1-x}N$ would be to attribute it as due to Fe^{2+} stabilized by nitrogen vacancies. However, the observed isomer shift ($\delta_{RT} \sim 0.27$ mm/s) is too low to justify this interpretation. For covalent Fe^{2+} on In sites, one would expect $\delta_{RT} \sim 0.7$ mm/s (with reference to

the results obtained in $Al_xGa_{1-x}N$). Therefore, alternative explanations have to be invoked, discussed below:

(a) *Doublet due to fast relaxing high-spin Fe^{3+}*: In order to have fast spin relaxations, the spins of the Fe^{3+} atoms have to couple to other spins in their immediate vicinity. Under the dilute conditions (<10^{-3} at.%) in the proposed experiments, interactions with other Fe^{3+} atoms are avoided [22]. A possible explanation could be interactions with spin-polarized vacancies as suggested by Coey *et al*. [23] in HfO_2. Such defect-related mechanism has been proposed to explain magnetism in systems where there are no 3*d* metal ions, but so far, no method has been able to verify this possibility on an atomic-scale.

(b) *Doublet due to low-spin Fe species*: Alternatively, one could consider low spin Fe species (the isomer shift is consistent with both low-spin Fe^{2+} and Fe^{3+}). However, this interpretation requires strong crystal field splitting, which does not seem feasible due to the longer bond-length in InN compared with $Al_xGa_{1-x}N$. If this is the case, it would make doping with other elements an attractive possibility for a dilute spin system.

(c) The possibility of *high-spin Fe^{2+}*, stabilized by nitrogen vacancies cannot be excluded, although it would not follow the expected behaviour of charge state and covalency.

(d) *Doublet due to interstitial Fe*: This possibility is also not attractive as we have no evidence for interstitial Fe in $Al_xGa_{1-x}N$, but cannot be excluded at this stage. In cubic III-Vs, recoil produced Fe interstitials were observed with an isomer shift, $\delta_{RT} \sim 1$ mm/s [24,25].

3. An additional component, Fe_Y was required to fit the spectral feature at $v \sim 0.83$ mm/s. The right leg of this component is not immediately observable, as it falls under the more intense single line component. However, representing this by a doublet (as in GaN) with isomer shift restricted to around 0.7 mm/s, results in the identification of this component as due to high-spin Fe^{2+}, presumably stabilized by V_N's in the neighbourhood of the probe atom. While this is the low intensity component in InN, it seem to be the dominating component in GaN, which could suggest that V_N is mobile in InN, while it is a stable defect in GaN [19].

2 Samples and Methods

2.1 InGaN samples

The available samples consist of single-crystal wurtzite (*wz*) $In_xGa_{1-x}N$ grown by metalorganic vapour phase epitaxy (MOVPE) on a 1 µm GaN buffer layer on *c*-plane sapphire. The layer is 600 nm thick. The samples are grown under H_2 atmosphere, with a pressure of 200 mbar and at a temperature of 850°C. The concentration of indium in the layers varies in the range $0 < x < 0.4$ and further series of samples with higher In concentrations are being prepared at Johannes Kepler University, Linz, Austria. Moreover, additional samples were obtained from Interuniversity Microelectronics Center (IMEC), Leuven, Belgium.

The structural, magnetic, electrical and optical properties of all samples will be preliminary investigated by means of: secondary ion mass spectroscopy (SIMS), energy dispersive X-ray spectroscopy (EDX), Raman spectroscopy, electron energy loss spectroscopy (EELS), high-resolution x-ray diffraction (HRXRD), high-resolution transmission electron microscopy (HRTEM), magnetotransport, photoluminescence (PL), SQUID magnetometry, electron paramagnetic resonance (EPR) and ferromagnetic resonance (FMR).

2.2 Emission Mössbauer Spectroscopy

In this project, we will predominantly utilise ^{57}Mn ($T_{½}$ = 1.5 min.) for ^{57}Fe eMS to study the charge and spin states of Fe in $In_xGa_{1-x}N$ samples. Mössbauer spectroscopy is particularly useful in this regard, given its sensitivity to the charge density and distribution in the immediate environment of the probe nucleus. Experiments with ^{57}Mn require local concentration <10^{-3} at.% were the probability of precipitation and interaction between Fe/Mn atoms are minimized. Thus, through hyperfine interactions, we can determine accurately the charge and spin states at the nucleus, which

can be related to the covalency of the probe environment and charge states of the Fe atom, in addition to the site symmetry. Consequently, we can easily identify magnetic components in the spectra, and from temperature dependent measurements, estimate the relaxation rates of high spin Fe^{3+}, as described by Mølholt *et al.* [26,27]. In addition, ^{119}In ($T_{½}$ = 2.1 min) and ^{57}Co ($T_{½}$ = 272 d) implantations will also be employed for online ^{119}Sn and offline ^{57}Fe eMS measurements.

The Mössbauer collaboration at ISOLDE/CERN [28] has access to all equipment needed.

The following measurements will be employed for different samples as a function of In/Ga ratios:

[M1] *Temperature series (^{57}Mn)*, where samples are measured at the low and high temperatures. This gives first indications of the annealing profile of the implantation induced damage (less intensity at increasing temperatures).

[M2] *Rapid-cooling experiments (^{57}Mn)*, where samples are rapidly cooled to liquid nitrogen temperatures (~110 K) [29], immediately after implantation at temperatures ≥ 300 K. The eMS measurements at this temperature present an ability to study low temperature effects which are usually desired after high temperature implantations. This approach can be used to address the effects of mobile defects and also enable the determination of Debye temperatures which are useful to support spectral component assignments.

[M3] *Angle dependent measurements (^{57}Mn)*, where samples are measured at different emission angles relative to the crystal axis. This method can easily distinguish between Fe in amorphous regions due to the implantation damage (no angular dependence) and Fe on regular lattice sites in non-cubic materials (angular dependence) [30]. Moreover, as a part of these measurements annealing on a minute time-scale is tested.

[M4] *^{119}In ($T_{½}$ = 2.1 min):* For specific compositions, it would be of interest to make use of ^{119}In implantations for ^{119}Sn eMS. This will give new information on the annealing of implantation damage, and knowledge concerning In-defect complexes and their stability.

[M5] *^{57}Co ($T_{½}$ = 272 d)*: For specific compositions, it would be of interest to make use of long lived ^{57}Co for ^{57}Fe eMS. It allows for wider range of external sample conditions and post treatment (for example annealing and irradiations) of samples than is possible with the short-lived isotopes (^{57}Mn and ^{119}In).

2.3 Complimentary studies

[C1] *Theoretical calculations.* To effectively explain the experimental results, *ab initio* density functional theory calculations for Fe in different lattice environments and charge states will be undertaken to compliment the experimental work proposed herein using the Wien2k package. This can aid in the identification of spectral components to specific defects, as reported for GeTe [31], In_2O_3 [32] and MgO [33].

[C2] *^{57}Fe implantations:* For selected samples, based on the results from the online eMS measurements (M1-M3), we can apply conversion electron Mössbauer spectroscopy (CEMS) on samples implanted with ^{57}Fe (<5 at.%) and (fx. at the University of the Witwatersrand and KU Leuven). These need higher fluences than utilized in eMS measurements following ^{57}Mn implantation, but can be applied to answer specific questions on the stability of different defects/implantation induced damage over longer annealing stages and also test different hypotheses.

[C3] *Other complimentary studies:* We have access to wide range of pre- and post-electrical, magnetization, and structural characterization techniques at different home institutions. Similar methods as used for pre-characterisation of grown samples, as well as ion beam related techniques can be applied depending on the findings.

[C4] *Emission channeling (EC):* The results on lattice sites, either substititutional, interstitial or Fe probe atoms in amorphous regions will be compared with results from emission channeling studies on end binary members, GaN [34] and InN [35] on using ^{59}Mn and ^{56}Mn, respectively.

Actual EC experiments on $In_xGa_{1-x}N$ for the different compositions, x are hindered by limitation on the analysis and/or simulations of different patterns for the alloys, since these are not easily achievable.

3 EXPECTATIONS FROM THE PROPOSED EXPERIMENTS

The experiments (M1-M5 and C2) proposed above are of interest in addressing possible interpretation of the different spectral components and their assignments as described in section 2.

- ✓ The effectivity of In to generate *p*-type doping will be established from the compositional dependence and/or fluence dependence (M1-3(x)), by following the development of spectral components. If defects seem to be responsible, irradiation of ^{57}Co (M5) or ^{57}Fe (C2) samples is possible. Investigations with Si doped samples (donor in nitrides) should assist as the introduction of donors in the layers counter-effects the *p*-type conductivity.
- ✓ If Fe_X is due to fast-relaxing high spin Fe^{3+}, we would expect to observe the spin-spin relaxation rate dependence on composition (M1-3(x)), allowing us to either support or reject this hypothesis. In addition, assuming that defect-free environments are formed upon implantation at elevated temperatures, rapid cooling (M2) will allow us to identify whether fast relaxation is a possible hypothesis.
- ✓ If Fe_X is due to low-spin configurations, the temperature dependence of the quadrupole interaction (M1) will reveal that. Here, we would employ angle dependent measurements (M3) to resolve the spectral lines where they otherwise overlap, and distinguish between Fe in crystalline sites and in (possible) amorphous regions (M5).
- ✓ The possibility that Fe_Y is due to high spin Fe^{2+} stabilized by nitrogen vacancies can be addressed by theoretical calculations (C1).
- ✓ The hypothesis that Fe_X is due to interstitial Fe can be addressed by rapid cooling experiments (M2) which allow for an unambiguous determination of Debye temperatures of the spectral components. This result will be inferred from previous emission channeling studies on GaN [34] and InN [35] as discussed in C4.

4 BEAM REQUEST/ISOTOPES

We envisage that 2-3 ^{57}Mn beam-times will be required. During the first beam-time, we will try to collect as much data as possible. Based on the results, the experimental program will be revised and optimized for the second run. If some outstanding questions remain, we may need to save some measurement time for the third beam opportunity. As highlighted in M1-M5, emission Mössbauer spectroscopy experiments proposed are listed in Table 1 with specific requests, in an attempt to address the scientific case presented here.

Table 1: Summary of proposes experiments.

Task	Isotopes	Time needed (hours)	Rationale
M1/M6	^{57}Mn, ^{119}In	28	~7 samples with different In/Ga ratios and with Si doping. Each full spectral series takes ~3.5 hours. At least two half temperature series with ^{119}In.
M2	^{57}Mn	10	For selected samples (~4), needs ~3 to 4 repeats and should be done at ~4 temperatures. Each measurement takes ~10 minutes.
M3/M4	^{57}Mn, (^{119}In)	8	Each measurement takes about an hour
M5	^{57}Co	16	If RILIS is not available, previous experience shows that at least 8 hours implantation time per sample is required.
Calibration	^{57}Mn, ^{119}In	9	~20%, based on experience
Contingency	^{57}Mn, ^{119}In, ^{57}Co	9	~20%, includes opportunistic science and possibilities of exploring new phenomena in greater depth

5 CONCLUSIONS/OUTLOOK

InN shows fascinating features and hyperfine parameters in ^{57}Fe emission Mössbauer spectroscopy experiments which are currently not well understood in relation to GaN (and $Al_xGa_{1-x}N$). Although $In_xGa_{1-x}N$ is an established building-block of commercially available devices, there are still many open questions on its fundamental electronic, magnetic and optical properties, some of which are addressed by our proposed experiment. Upon completion of the proposed experimental activities, we will have identified information on the lattice sites, Fe charge and spin states in these systems. We are very optimistic that with the proposed experiments, we will gain a deep understanding of the physics that underpins the peculiar functionalities of $In_xGa_{1-x}N$, which can result in a wide range of investigation/perspectives for the next generation of opto-electronic, photovoltaic and spintronic devices.

6 SUMMARY OF REQUESTED SHIFTS

Table 2: Isotopes, intensities, energies and shifts requested.

Isotope	Minimum Intensity/μC	Energy	Shifts	Target	Ion source	Notes
^{57}Mn (1.5 min)	(2-3)×10^8	≥ 50 keV	7	UC_x	Mn RILIS	
^{57}Co ($T_{½}$ = 272 d)	1×10^7	≥ 50 keV	2	ZrO_2 or YtO_2	Co RILIS	A
^{119}In (2.1 min)	(2-3)×10^8	≥ 50 keV	1	UC_x	In RILIS	B
Total			**10**			

A: ^{57}Ni (38 h → ^{57}Co) RILIS could be an option

B: We will make a short ^{111}In collection to test the feasibility of using perturbed angular correlation spectroscopy measurement.

7 REFERENCES

[1] Smeeton, T. and Humphreys, C.: Perspectives on Electronic and Optoelectronic Materials. In Kasap, s. and Capper, P., eds., *Springer Handbook of Electronic and Photonic Materials*. Springer, 2007.

[2] Vurgaftman, I., Meyer, J.R., and Ram-Mohan, L.R.: *J. Appl. Phys.*, **89** (2001) 5815.

[3] Wu, J., Walukiewicz, W., Yu, K.M., J.W.Ager, Haller, E.E., Lu, H., Schaff, W. J., Saito, Y., and Nanishi, Y.: *Appl. Phys. Lett.*, **80** (2002) 3967.

[4] Nakamura, S.: *Rev. Mod. Phys.*, **87** (2015) 1139.

[5] Nakamura, S., Pearton, S., and Fasol, G.: *The Blue laser Diode - The Complete Story*. Springer-Verlag , Berlin, Heidelberg, 2000.

[6] Xu, D.: *Multi-dimensional Optical Storage*. Springer and Tsinghua University Press, Singapore, 2016.

[7] *http://www.nobelprize.org/nobel_prizes/physics/laureates/2014/*.

[8] Janotti, A. and Van de Walle, C. G.: Theory of native point defects and impurities in InN. In Veal, T. D., McConville, C. F., and Schaff, W. J., eds., *Indium Nitride and Related Alloys*. CRC Press, Boca Raton London New York, 2010.

[9] Collazo, R. and Dietz, N.: The Group III-Nitrides Materials Class: from Preparation to Perspectives in Photoelectrocatalysis. In Lewerenz, H-J., Peter, L., and Zhao, T.S., eds., *Photoelectrochemical Water Splitting: Materials, Processes and Architectures*. The Royal Society of Chemistry, Cambridge, 2013.

[10] Lester, S. D., Ponce, F. A., Craford, M. G., and Steigerwald, D. A.: *Appl. Phys. Lett. 66*, **669** (1995) 1249.

[11] Chichibu, S., Azuhata, T., Sota, T., and Nakamura, S.: *Appl. Phys. Lett.*, **69** (1996) 4188.

[12] Nakamura, S.: *Science*, **281** (1998) 956.

[13] Browne, D., Mazumder, A., B., Wu, Y.-R., and Speck, J. S.: *J. Appl.Phys.*, **117** (2015) 185703.

[14] Nakamura, S., Iwasa, N., Senoh, M., and Mukai, T.: *Jpn. J. Appl. Phys.*, **31** (1992) 1258.

[15] Nakamura, S., Mukai, T., Senoh, M., and Iwasa, N.: *Jpn. J. Appl. Phys.*, **31** (1992) L139.

[16] Gunnlaugsson, H. P., Mølholt, T. E., Mantovan, R., Masenda, H, Naidoo, D., Dlamini, W.B., Sielemann, R., Bharuth-Ram, K., Fanciulli, M., Gíslason, H.P., Johnston, K., Kobayashi, Y., Langouche, G., Ólafsson, S., Yoshida, Y., Weyer, G., and Decoster, S.: *Emission Mössbauer spectroscopy of advanced materials for opto- and nano- electronics*. Geneva, ISOLDE/CERN, [Proposal Sumbitted to INTC] 2013.

[17] Bonanni, A., Gunnlaugsson, H. P., Mantovan, R., Masenda, H., Bharuth-Ram, K., Gíslason, H. P., Johnston, K., Langouche, G., Moodley, M., Mølholt, T. E., Naidoo, D., Ncube, M., Ólafsson, S., Pereira, L. C. M., and A. Svane, A.: *Magnetic and structural properties of manganese doped (Al,Ga)N studied with Emission Mössbauer spectroscopy*. Geneva, ISOLDE/CERN, [Proposal Sumbitted to INTC] 2013.

[18] Gunnlaugsson, H. P., Mølholt, T. E., Mantovan, R., Masenda, H., Naidoo, D., Dlamini, W. B., Sielemann, R., Bharuth-Ram, K., Weyer, G., Johnston, K., Langouche, G., Ólafsson, S., Gíslason, H. P., Kobayashi, Y., Yoshida, Y., Fanciulli, M., and the ISOLDE Collaboration.: *Appl. Phys. Lett.*, **97** (2010) 142501.

[19] Masenda, H., Naidoo, D., Bharuth-Ram, K., Gunnlaugsson, H.P., Johnston, K., Mantovan, R, Mølholt, T.E., Ncube, M, Shayestehaminzadeh, S., Gíslason, H.P., Langouche, G., Ólafsson, S., and Weyer, G.: *J. Magn. Magn. Mater.*, **401** (2016) 1130.

[20] Dietl, T., Ohno, H., Matsukura, F., Cibert, J., and Ferrand, D.: *Science*, **287** (2000) 1019.

[21] Dietl, T.: *Nature. Mater.*, **9** (2010) 965.

[22] Mantovan, R., Gunnlaugsson, H. P., Johnston, K., Masenda, H., Mølholt, T. E., Naidoo, D., Ncube, M., Shayestehaminzadeh, S., Bharuth-Ram, K., Fanciulli, M., Gíslason, H. P, Langouche, G., Ólafsson, S., Pereira, L. M. C., Wahl, U., Torelli, P., and Weyer, G.: *Adv. Electron. Mater.*, **1** (2015) 1400039.

[23] Coey, J.M.D., Venkatesan, M., Stamenov, P., Fitzgerald, C. B., and Dorneles, L. S.: *Phys. Rev. B*, **72** (2005) 024450.

[24] Masenda, H., Naidoo, D., Bharuth-Ram, K., Gunnlaugsson, H. P., Weyer, G., Dlamini, W. B., Mantovan, R., Sielemann, R., Fanciulli, M., Mølholt, T. E., Ólafsson, S., Langouche, G., Johnston, K., and the ISOLDE Collaboration.: *Hyp. Int.*, **198** (2010) 15.

[25] Bharuth-Ram, K., Dlamini, W. B., Masenda, H., Naidoo, D., Gunnlaugsson, H. P., Weyer, G., Mantovan, R., Mølholt, T. E., Sielemann, R., Ólafsson, S., Langouche, G., Johnston, K., and the ISOLDE Collaboration.: *Nucl. Instr. Meth. B*, **272** (2011) 414.

[26] Mølholt, T. E., Mantovan, R., Gunnlaugsson, H. P., Naidoo, D., Ólafsson, S., Bharuth-Ram, K., Fanciulli, M., Johnston, K., Kobayashi, Y., Langouche, G., Masenda, H., Sielemann, R., Weyer, G., and Gíslason, H. P.: *Hyp. Int.* , **197** (2010) 89.

[27] Mølholt, T. E, Gunnlaugsson, H. P., Johnston, K, Mantovan, R., Masenda, H., Naidoo, D., Ólafsson, S., Bharuth-Ram, K., Gislason, H. P., Langouche, G., Sielemann, R., Weyer, G., and the ISOLDE Collaboration.: *Phys. Scr.*, **T148** (2012) 014006.

[28] *e-ms.web.cern.ch*.

[29] Gunnlaugsson, H.P. and al, et. Annealing studies in emission Mössbauer spectroscopy using short lived isotopes.: *Manuscript in preparation* (2016).

[30] Gunnlaugsson, H. P., Johnston, K., Mølholt, T. E., Weyer, G., Mantovan, R., Masenda, H., Naidoo, D., Ólafsson, S., Bharuth-Ram, K., Gíslason, H. P., Langouche, G., Masden, M. B., and the ISOLDE Collaboration.: *Appl. Phys. Lett.*, **100** (2012) 042109.

[31] Mantovan, R., Fallica, R, Gerami, A.G., Mølholt, T. E., Wiemer, C., Longo, M., Gunnlaugsson, H. P., Johnston, K., Masenda, H., Naidoo, D., Ncube, M., Bharuth-Ram, K., Fanciulli, M., Gíslason, H. P, Langouche, G., Ólafsson, S., and Weyer, G. Atomic-scale study of the amorphous-to-crystalline phase transition mechanism in GeTe.: *under review* (2016).

[32] Gerami, A.M., Johnston, K., Gunnlaugsson, H. P., Nomura, K., Mantovan, R., Masenda, H., Matveyev, A., Mølholt, T.E., Ncube, M., Shayestehaminzadeh, S., Unzueta, I., Gislason, H.P., Krastev, P. B., Langouche, G., Naidoo, D., and Ólafsson, S.: *Hyp. Int.*, **237** (2016) 75.

[33] Mølholt, T. E., Mantovan, R., Gunnlaugsson, H. P., Svane, A., Masenda, H., Naidoo, D., Bharuth-Ram, K., Fanciulli, M., Gíslason, H. P., Johnston, K., Langouche, G., Ólafsson, S., Sielemann, R., and Weyer, G.: *J. Appl. Phys.*, **115** (2014) 023502.

[34] Wahl, U., Vantomme, A., Langouche, G., Correia, J.G., Peralta, L., and Collaboration, The ISOLDE.: *Appl. Phys. Lett.*, **78** (2001) 3217.

[35] Amorim, L.: *Lattice site location of electrical dopant impurities in group-III nitrides, in preparation*. KU Leuven, Leuven, 2016.

Appendix

DESCRIPTION OF THE PROPOSED EXPERIMENT

The experimental setup comprises: *(name the fixed-ISOLDE installations, as well as flexible elements of the experiment)*

Part of the Choose an item.	Availability	Design and manufacturing
Mössbauer Set-up	☒ Existing	☒ To be used without any modification
SSP-GLM chamber	☒ Existing	☒ To be used without any modification ☐ To be modified
	☐ New	☐ Standard equipment supplied by a manufacturer ☐ CERN/collaboration responsible for the design and/or manufacturing

HAZARDS GENERATED BY THE EXPERIMENT

(if using fixed installation) Hazards named in the document relevant for the fixed [COLLAPS, CRIS, ISOLTRAP, MINIBALL + only CD, MINIBALL + T-REX, NICOLE, SSP-GLM chamber, SSP-GHM chamber, or WITCH] installation.

Additional hazards:

Hazards			
	Mössbauer setup (online experiments)	*SSP-GLM chamber*	*[Part 3 of the experiment/equipment]*
Thermodynamic and fluidic			
Pressure	Low pressure only	Low pressure only	
Vacuum	Yes	Yes	
Temperature	< 100°C (outside setup)	Room temperature	
Heat transfer	No	No	
Thermal properties of materials	Metal	N/A	
Cryogenic fluid	N_2, 1[Bar], 3 l/h	N/A	
Electrical and electromagnetic			
Electricity	<20 V, < 20 A	None	
Static electricity	None	None	
Magnetic field	< 0.1 T (outside setup)	None	
Batteries	☐		
Capacitors	☐		
Ionizing radiation			
Target material	Diverse	Diverse	
Beam particle type (e, p, ions, etc)	Ions	Ions	
Beam intensity	$<10^9$ s^{-1}	$<10^9$ s^{-1}	
Beam energy	>50 keV	>50 keV	
Cooling liquids	[liquid]		
Gases	[gas]		
Calibration sources:	☐		
• Open source	☐		
• Sealed source	☐ [ISO standard]		
• Isotope			
• Activity			
Use of activated material:			
• Description	☐		

• Dose rate on contact and in 10 cm distance	^{57}Mn (estimated) @ 10cm 150 μSV/hr Similar for ^{119}In Concrete shielding employed around implantation chamber	0.04 μSv/hr @ 10cm for 0.4MBq	
• Isotope	^{57}Mn, ^{119}In	^{57}Co	
• Activity	~50 mCi (inside the setup) (185 MBq)	4-10 µCi (0.15-0.4 MBq)	
Non-ionizing radiation			
Laser			
UV light	No	No	
Microwaves (300MHz-30 GHz)	No	No	
Radiofrequency (1-300MHz)	No	No	
Chemical			
Toxic	No	No	
Harmful	No	No	
CMR (carcinogens, mutagens and substances toxic to reproduction)	No	No	
Corrosive	No	No	
Irritant	No	No	
Flammable	No	No	
Oxidizing	No	No	
Explosiveness	No	No	
Asphyxiant	No	No	
Dangerous for the environment	No	No	
Mechanical			
Physical impact or mechanical energy (moving parts)	No	No	
Mechanical properties (Sharp, rough, slippery)	No	No	
Vibration	No	No	
Vehicles and Means of Transport	No	No	
Noise			
Frequency	No	No	
Intensity	No	No	
Physical			
Confined spaces	No	No	
High workplaces	No	No	
Access to high workplaces	No	No	
Obstructions in passageways	Just outside GLM	No	
Manual handling	[location]		
Poor ergonomics	[location]		

0.1 Hazard identification

3.2 Average electrical power requirements (excluding fixed ISOLDE-installation mentioned above): *(make a rough estimate of the total power consumption of the additional equipment used in the experiment)*